Surfactant functionalization induces robust, differential adhesion of tumor cells and blood cells to charged nanotube-coated biomaterials under flow

Michael J. Mitchell [a, b, 1], Carlos A. Castellanos [a, 1], Michael R. King [a, *]

[a] Department of Biomedical Engineering, Cornell University, Ithaca, NY 14853, USA
[b] David H. Koch Institute for Integrative Cancer Research, Department of Chemical Engineering, Massachusetts Institute of Technology, Cambridge, MA 02139, USA

ARTICLE INFO

ABSTRACT

The metastatic spread of cancer cells from the primary tumor to distant sites leads to a poor prognosis in cancers originating from multiple organs. Increasing evidence has linked selectin-based adhesion between circulating tumor cells (CTCs) and endothelial cells of the microvasculature to metastatic dissemination, in a manner similar to leukocyte adhesion during inflammation. Functionalized biomaterial surfaces hold promise as a diagnostic tool to separate CTCs and potentially treat metastasis, utilizing antibody and selectin-mediated interactions for cell capture under flow. However, capture at high purity levels is challenged by the fact that CTCs and leukocytes both possess selectin ligands. Here, a straightforward technique to functionalize and alter the charge of naturally occurring halloysite nanotubes using surfactants is reported to induce robust, differential adhesion of tumor cells and blood cells to nanotube-coated surfaces under flow. Negatively charged sodium dodecanoate-functionalized nanotubes simultaneously enhanced tumor cell capture while negating leukocyte adhesion, both in the presence and absence of adhesion proteins, and can be utilized to isolate circulating tumor cells regardless of biomarker expression. Conversely, diminishing nanotube charge via functionalization with decyltrimethylammonium bromide both abolished tumor cell capture while promoting leukocyte adhesion.

© 2015 Elsevier Ltd. All rights reserved.

1. Introduction

Metastasis, the spread of cancer cells from a primary tumor to anatomically distant organs, contributes to over 90% of cancer-related deaths [1]. Cancer cells shed from the primary tumor, which can number as many as one million cells per gram of tumor per day [2,3], enter the bloodstream as circulating tumor cells (CTCs) via the process of intravasation [4,5]. Once in blood, CTCs must withstand fluid shear forces and immunological stress to translocate to microvessels in anatomically distant organs [6,7]. CTCs adhesively interact with receptors on the endothelial cell wall under flow, in a manner similar to the leukocyte adhesion cascade involved in inflammation and lymphocyte homing to lymphatic tissues [8,9]. Recent work has shown that CTCs display glycosylated ligands similar to leukocytes, which can trigger the initial adhesion with selectin receptors on the endothelium [10,11]. Due to their rapid, force-dependent binding kinetics, selectins can initiate CTC rolling adhesion along the blood vessel wall [12,13]. CTCs transition from rolling to eventual firm adhesion, allowing for transmigration into tissues and the formation of secondary tumors [14]. While surgery, radiation, and chemotherapy have proven generally successful at treating primary tumors that do not invade the basement membrane, the difficulty of detecting distant micrometastases has made the majority of metastatic cancer treatments ineffective. As a means to combat metastasis, approaches are currently being explored to target and kill CTCs in the bloodstream before the formation of secondary tumors [15—18]. Additionally, methods are being developed to isolate CTCs at high purity levels from patient blood, for the development of personalized medicine regimens for those with metastatic cancer [19—21].

CTCs are sparsely distributed in the bloodstream, with CTC concentrations as low as 1–100 cells/mL [22]. Their separation and isolation from blood is commonly referred to as a "needle in a haystack problem", as leukocytes and erythrocytes are present in concentrations of one million and one billion cells per milliliter of blood, respectively [7,23]. Thus, numerous techniques for CTC isolation are in development, including magnetic bead-based CTC separation assays [24], flow-based microfluidic platforms for rapid isolation of CTCs from whole blood [25,26], and devices to separate tumor cells based on their chemotactic phenotype [27]. Our lab has recently developed microscale flow devices that mimic the metastatic adhesion cascade process to capture and separate CTCs from whole blood under flow conditions. Utilizing surfaces coated with recombinant human E-selectin (ES) and antibodies against the CTC markers epithelial cell adhesion molecule (EpCAM) and prostate-specific membrane antigen (PSMA), we have fabricated flow devices to rapidly separate viable CTCs from patient blood and deliver targeted chemotherapeutics to cancer cells [26,28]. However, improvement of current CTC isolation purity levels is challenged by the fact that both CTCs and leukocytes express ES ligands [8].

Halloysite nanotubes (HNT) are naturally occurring clay minerals that are typically 800 ± 300 nm in length, 50–70 nm in outer diameter, and 10–30 nm in inner diameter [29]. Halloysite ($Al_2Si_2O_5(OH)_4$) is a two-layered (1:1) aluminosilicate that consists of an external siloxane (Si–O–Si) surface and an internal aluminol (Al–OH) surface [30]. At physiological pH, HNT has a negatively charged outer surface and a positively charged inner lumen [31], which has been exploited for the encapsulation and sustained release of drugs such as Nifedipine, Furosemide, and dexamethasone [32]. The differences in HNT surface charge have also been exploited for the selective adsorption of anionic and cationic surfactants, which significantly alters HNT zeta potential [33]. Our lab has shown that HNT-coated biomaterials of nanoscale roughness can increase surface area and thus selectin protein adsorption [34], which can enhance selectin-mediated cancer cell capture. Herein, we present the use of HNT in combination with cationic and anionic surfactants to develop nanostructured biomaterials that differentially adhere tumor cells and leukocytes under flow conditions.

2. Materials and methods

2.1. Cell culture

Human colon adenocarcinoma COLO 205 (ATCC #CCL-222), breast adenocarcinoma MCF7 (ATCC #HTB-22), and breast adenocarcinoma MDA-MB-231 (ATCC #HTB-26) cell lines were purchased from American Type Culture Collection (ATCC; Manassas, VA, USA). COLO 205 and MDA-MB-231 cells were grown in RPMI 1640 supplemented with 10% fetal bovine serum (FBS) and 1% PenStrep (PS), all purchased from Invitrogen (Grand Island, NY, USA). MCF7 cells were cultured in Eagle's Minimum Essential Medium supplemented with 0.01 mg/mL bovine insulin, 10% FBS, and 1% PenStrep, all purchased from Invitrogen. Both cell lines were incubated under humidified conditions at 37 °C and 5% CO2, and were not allowed to exceed 90% confluence. In preparation for capture assays, cancer cells were removed from culture via treatment with Accutase (Sigma–Aldrich, St. Louis, MO, USA) for 10 min prior to handling. All cells were washed in HBSS, and resuspended at a concentration of 1.0×10^6 cells/mL in HBSS flow buffer supplemented with 0.5% HSA, 2 mM Ca^{2+}, and 10 mM HEPES (Invitrogen), buffered to pH 7.4.

2.2. Polymorphonuclear (PMN) cell isolation

Human neutrophils were isolated as described previously [35,36]. Human peripheral blood was collected from healthy blood donors via venipuncture after informed consent and stored in heparin containing tubes (BD Biosciences, San Jose, CA, USA). Blood was carefully layered over 1-Step™ Polymorphs (Accurate Chemical and Scientific Corporation, Westbury, NY, USA) and separated via centrifugation using a Marathon 8K centrifuge (Fisher Scientific, Pittsburgh, PA, USA) at 1800 rpm for 50 min. Polymorphonuclear (PMN) cells, also known as neutrophils, were extracted and washed in cation-free HBSS, and excess red blood cells were lysed hypotonically. Prior to capture assays, neutrophils were resuspended in HBSS flow buffer supplemented with 0.5% human serum albumin (HSA), 2 mM Ca^{2+}, and 10 mM HEPES (Invitrogen), buffered to pH 7.4.

2.3. Halloysite nanotube functionalization

Halloysite nanotubes (HNT; NaturalNano, Rochester, NY, USA) were added to water to a final concentration of 6.6% (w/v). 1.6 g HNT was added to 100 mL of 0.1 M aqueous sodium dodecanoate (NaL) and 2.4 g HNT were added to 100 mL of 0.1 M aqueous decyl trimethyl ammonium bromide (DTAB; Sigma–Aldrich) and mixed using a magnetic stirrer for 48 h. Surfactant-treated nanotubes were then washed several times in water and allowed to dry overnight. Untreated HNT were kept in water at a concentration 6.6% (w/v). NaL and DTAB-treated HNT were stored in water or methanol respectively, to a final concentration of 6.6% (w/v). To evaluate adsorption of surfactants to HNT, the hydrodynamic radius (nm) and zeta potential (mV) of HNT, NaL-HNT, and DTAB-HNT were measured by dynamic light scattering (DLS) using a Malvern Zetasizer Nano ZS (Malvern Instruments Ltd., Worcestershire, UK). Treated and untreated nanotubes at a concentration of 0.37% (w/v) were prepared prior to DLS measurements, using the same solvents as described above for functionalized and untreated HNT samples. To assess the effect of ES adsorption on HNT zeta potential, 0.5 mL of HNT, NaL-HNT, and DTAB-HNT at a concentration of 1.1% (w/v) were centrifuged at 13,000 rpm for 10 min and incubated with 0.5 mL of ES at a concentration of 2.5 μg/mL for 2.5 h at RT. All samples were centrifuged at 13,000 rpm for 10 min and resuspended in water at the same concentration used for HNT measurements in the absence of ES. Colloidal stability of treated and untreated HNT was assessed by allowing samples of treated and untreated HNT to settle for 24 h after mixing.

2.4. Fabrication of nanostructured HNT surfaces

Microrenathane (MRE) tubing (Braintree Scientific, Braintree, MA, USA) of inner diameter 300 μm was cut to 55 cm in length and fastened onto the stage of an Olympus IX-71 inverted microscope (Olympus, Center Valley, PA, USA). Ethanol was rinsed through the tubes using a motorized syringe pump (KDS 230; IITC Life Science, Woodland Hills, CA, USA) at a flow rate of 1 mL/min. To functionalize the inner MRE surface with HNT, microtubes were washed thoroughly with distilled water, followed by incubation with poly-L-lysine solution (0.02% w/v in water) for 5 min and incubation with untreated or NaL-functionalized HNT (NaL-HNT, 1.1% w/v) for 5 min. To functionalize the surface with DTAB-treated HNT (DTAB-HNT), aqueous 2:8 L-glutamic acid (0.1% w/v, Sigma) was incubated in microtubes for 5 min, prior to incubation with DTAB-HNT (1.1% w/v) for 5 min. Microtubes were then washed thoroughly with distilled water at 0.02 mL/min to remove non-adsorbed halloysite, and cured overnight at room temperature (RT). To immobilize ES adhesion protein to HNT-coated surfaces, recombinant human ES/Fc chimera (rhE/Fc) (R&D Systems, Minneapolis, MN, USA) at a concentration of 2.5 μg/mL was perfused through microtubes at 0.02 mL/min. ES was incubated for 2.5 h at RT within HNT-coated microtubes and smooth microtubes in the absence of HNT. In some experiments, HNT-coated surfaces were utilized in the absence of ES. All surfaces were blocked for nonspecific cell adhesion for 1 h via perfusion and incubation with 5% (w/v) bovine serum albumin (BSA, Sigma–Aldrich) at 0.02 mL/min. ES protein was activated with calcium enriched flow buffer for 5 min prior to cell capture experiments.

2.5. ES surface adsorption assay

To characterize ES adsorption on smooth and immobilized HNT surfaces, anti-human CD62E (BD Biosciences, San Jose, California, USA) conjugated to an allophycocyanin (APC) fluorophore was perfused through microtubes at 0.02 mL/min and incubated for 2.5 h at RT, following incubation with ES protein and BSA as described above. Unbound ES antibodies were washed from surfaces using flow buffer. Fluorescent images of adsorbed ES on surfaces were acquired at 90× magnification using an IX-81 inverted microscope linked to a Hitachi CCD camera (Hitachi, Japan). Fluorescent images were analyzed using a three dimensional (3D) surface plot plug-in for ImageJ to obtain pixel intensity data.

2.6. HNT surface characterization

To characterize immobilized HNT surfaces, 100 μL of 1.1% untreated HNT, NaL-HNT, and DTAB-HNT solutions were carefully dried on 3 cm × 3 cm polyurethane (PU) sheets (Thermo Scientific, USA) and sputter coated with Au prior to visualization. SEM images of untreated HNT, NaL-HNT, and DTAB-HNT immobilized onto PU surfaces were acquired with the Leica Stereoscan 440 scanning electron microscope (Leica Microsystems Gmbh, Wetzlar, Germany). For atomic force microscopy (AFM) measurements, flat samples of HNT-coated surfaces were prepared on polystyrene microscope slides (Thermo Fisher Scientific, Rochester, NY, USA) using an 8-well flexiPERM gasket (Sigma–Aldrich) following the same method used for microtube functionalization. Samples were then imaged using a Veeco DI-3000 AFM (Veeco Instruments, Inc., Woodbury, NY, USA). 10 μm × 10 μm images were recorded at random locations on each sample. Three images each of the flat HNT-coated samples and untreated surfaces were analyzed in WSxM 5.0 software [37] to inspect the surface height profiles and root-mean-square surface roughness.

2.7. Cell capture assays

Cell suspensions were perfused through microtubes using a motorized syringe pump and monitored via an inverted microscope linked to a Hitachi CCD KP-M1AN camera (Hitachi, Japan) and a Sony DVD Recorder DVO-1000MD (Sony Electronics Inc., San Diego, California, USA). Cancer cells were perfused at 0.008 mL/min (wall shear stress of 0.5 dyn/cm^2) for 15 min, and then 0.04 mL/min (wall shear stress of 2.5 dyn/cm^2) for 45 min. Polymorphonuclear neutrophils were perfused through microtubes at 0.04 mL/min for 60 min. Mixtures of cancer cells and leukocytes at cancer cell:leukocyte ratios of 1:1 and 1:10 were perfused through microtubes at 0.04 mL/min for 60 min. The number of adhered cells was taken from ten random video frames for each microtube.

2.8. Statistical analysis

Data sets were plotted and analyzed using Microsoft Excel (Microsoft, Redmond, WA, USA) and GraphPad Prism 5.0 (GraphPad software, San Diego, CA, USA). All results were reported as the mean ± standard error of the mean (SEM) or standard deviation (SD) as indicated. Two-tailed paired and unpaired t-tests, and one-way ANOVA with Tukey post-tests were utilized for statistical analyses. P-values less than 0.05 were considered significant.

3. Results

We are interested in exploiting the negatively charged outer surface and positively charged inner lumen of HNT to alter surface charge via simple surfactant functionalization (Fig. 1A), while maintaining HNT surfaces of nanoscale roughness, to differentially capture cancer cells and blood cells via ES adhesion proteins under flow conditions (Fig. 1B). Due to the negatively charged outer surface and positively charged inner lumen of HNT, we sought to manipulate the nanotube charge using both positive and negatively charged surfactants (Fig. 1A). Sodium dodecanoate (NaL) and decyl trimethyl ammonium bromide (DTAB) were used to neutralize the positive inner lumen and the negative outer surface charge, respectively (Fig. 1A). NaL and DTAB possess negative and positive functional head groups, respectively, which are needed to bind to the surface and inner lumen of HNT [33]. The aqueous dispersibility of HNT is affected by both hydrophobic interactions and electrostatic effects [33]. Functionalization of HNT by mixing with NaL (NaL-HNT) for 48 h formed stable aqueous dispersions (Fig. 1C), and possessed a negative zeta potential greater than that of untreated HNT (Fig. 1D). These results are consistent with the idea that NaL molecules penetrate within HNT and neutralize the positive charge within the nanotube lumen. Additionally, the increase in negative nanotube charge due to NaL treatment allows the nanotubes to interact with water via charge—dipole interactions.

Conversely, functionalization of HNT with DTAB (DTAB-HNT) via mixing for 48 h diminished the intrinsic negative charge of HNT (Fig. 1D), with polar head groups of DTAB neutralizing external negative charges. At the same time, the long hydrocarbon chain of DTAB is left exposed to solvent water molecules. For DTAB-HNT to disperse in water, non-polar chains must move between water molecules, substituting their weak attractions for strong hydrogen bonds among water molecules [38]. Unable to substitute for intermolecular hydrogen bonds, and aggregating due to hydrophobic forces, DTAB-HNT quickly sediment in a manner similar to untreated HNT (Fig. 1C). Adsorption of ES adhesion receptors to HNT, NaL-HNT, and DTAB-HNT altered charge minimally, by ~2—5 mV (Fig. 1D).

Functionalized HNT can then be immobilized in polyurethane microtubes to create HNT-coated surfaces of nanoscale roughness (Fig. 1B). To evaluate the effect of surfactant treatment on the immobilization of HNT to form surfaces of nanoscale roughness, we characterized both treated and untreated HNT samples immobilized on polyurethane sheets using scanning electron microscopy (SEM). Larger polyurethane sheets were used for analysis rather than microtubes to minimize sample damage during handling and preparation. Poly-L-lysine (PLL) coatings were used to immobilize HNT and NaL-HNT, with the negatively-charged HNT and NaL-HNT being attracted to the positively-charged PLL coating via electrostatic interactions. Conversely, negatively-charged glutamic acid coatings were used to immobilize DTAB-HNT. SEM images revealed that, regardless of surfactant treatment, HNT immobilization creates filamentous surfaces, with HNT protruding from all surfaces (Fig. 1E). AFM images also confirmed that immobilized HNT samples all displayed tubular structures protruding outward from the surfaces at varying feature heights, regardless of surfactant treatment (Fig. 1F, G). Root mean square (RMS) roughness values of all HNT-coated surfaces were within the range of 140—200 nm (Fig. 1H). This range of roughness has previously been shown to enhance cancer cell adhesion via increasing formation of focal adhesion complexes [39]. These data suggest that simple surfactant mixing can functionalize and alter HNT charge, without effecting the immobilization of HNT to create surfaces of nanoscale roughness.

To evaluate the effects of functionalized HNT surfaces (Fig. 2A) on the adsorption of ES receptors, ES was immobilized on smooth, untreated, and treated HNT surfaces and labeled with fluorescent ES antibodies to determine protein fluorescence intensity. Fluorescence micrographs indicated that ES was immobilized on smooth (Fig. 2B), NaL-HNT (Fig. 2C), untreated HNT (Fig. 2D), and DTAB-HNT (Fig. 2E). Quantification of surface fluorescence intensity showed that untreated and treated HNT surfaces increased ES adsorption, with all HNT surfaces possessing significantly greater average ES fluorescence intensities than smooth surfaces (Fig. 2F). Enhanced ES adsorption to HNT surfaces is likely due to the increase in surface area created by HNT immobilization, previously shown by our lab to increase protein adsorption [34]. Differences in ES adsorption on treated and untreated HNT could be due to changes in HNT surface charge, since differences in surface roughness were minimal (Fig. 1H) and thus surface area differences between HNT surfaces are likely negligible. With an isoelectric point at pH 5.2, ES assumes a net negative charge at physiologic pH. Decreased ES adsorption on NaL-HNT compared to other HNT surfaces is thus likely due to electrostatic repulsion between ES and NaL-HNT, both negatively charged. These results indicate that HNT immobilization to biomaterial surfaces enhances ES adsorption.

We then investigated the use of nanostructured surfaces of negatively charged NaL-HNT to facilitate capture of flowing tumor cells and leukocytes via ES-mediated adhesion. Our lab has previously developed reactive biomaterial surfaces that have been utilized for the study of leukocyte, stem cell, and tumor cell adhesive interactions with selectins under flow [13,40,41]. Colorectal adenocarcinoma COLO 205 and breast adenocarcinoma MCF7 cells were used in these experiments as model CTCs because they possess ligands for ES, are known to interact with ES under physiological shear stresses [42,43], and form metastases in vivo [44—46]. As expected, COLO 205 cells adhesively interacted with nanostructured HNT surfaces consisting of immobilized ES (ES + HNT) under flow (Fig. 3A), at a physiological flow rate of 0.04 mL/min (wall shear stress (WSS) = 2.5 dyn/cm^2). Interestingly, increasing the negative charge of HNT with NaL surfactant dramatically increased the number of COLO 205 cells recruited via ES under flow (Fig. 3A), compared to untreated HNT-coated surfaces. Enhancement of HNT charge with NaL increased the number of COLO 205 cancer cells captured from flow by ~150%, compared to surfaces comprised of HNT without surfactant treatment (Fig. 3B). Capture of breast MCF7 cancer cells from flow on NaL-HNT surfaces increased by over 800% compared to HNT surfaces without surfactant treatment, demonstrating that this approach can be utilized to target and capture tumor cells from multiple organs (Fig. 3C).
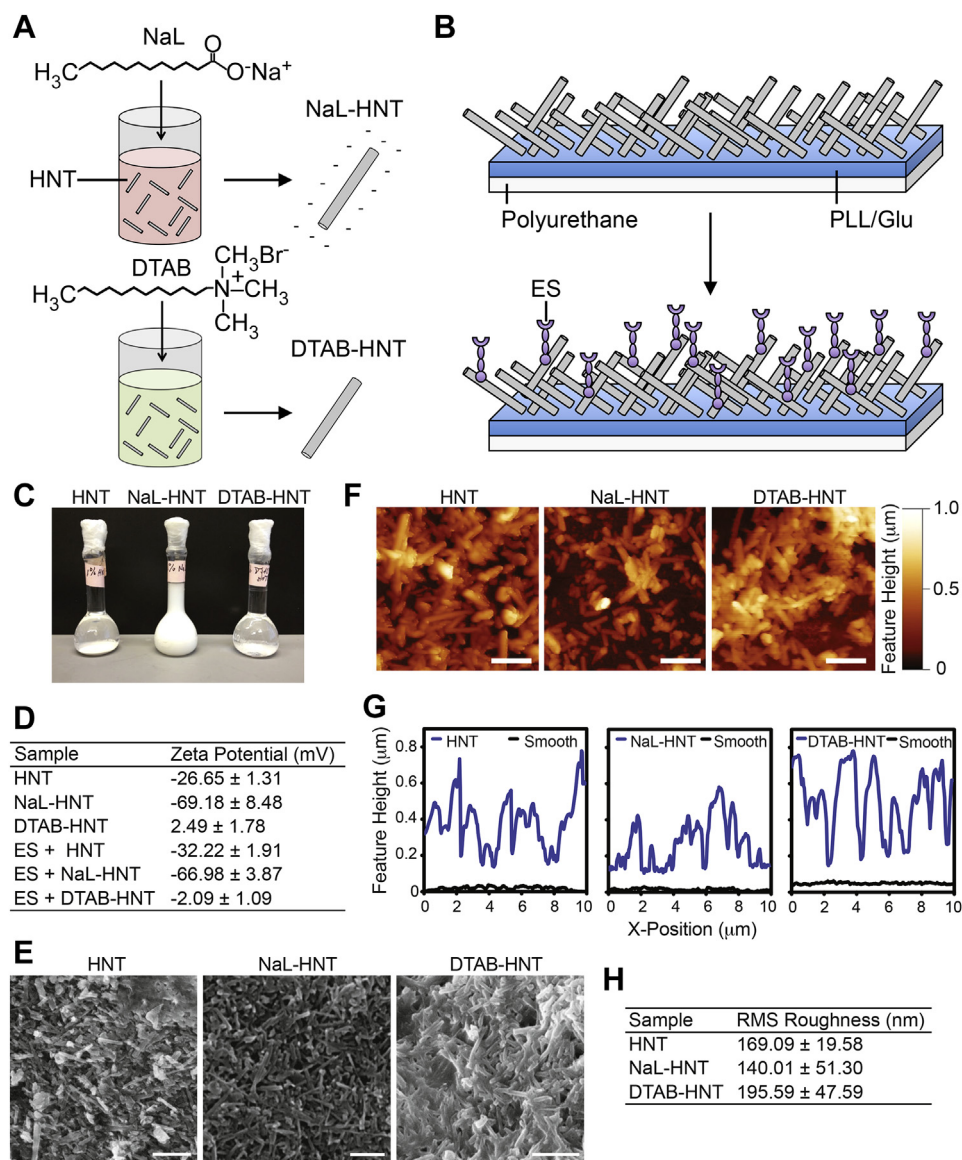
Fig. 1. Functionalization of halloysite nanotubes (HNTs) with surfactants to fabricate nanostructured surfaces of altered surface charge for flow-based cell capture assays. (A) Negative charge of HNT is enhanced via mixing and functionalization with sodium dodecanoate (NaL) surfactant (NaL-HNT). Intrinsic negative charge of HNT is attenuated via mixing and functionalization of decyltrimethylammonium bromide (DTAB) surfactant (DTAB-HNT). (B) HNTs are immobilized onto polyurethane flow device surfaces coated with poly-L-lysine (for HNT and NaL-HNT) or glutamic acid (for DTAB-HNT) for cell capture assays. Surfaces can be further functionalized with adhesion proteins, such as E-selectin (ES) to facilitate cell capture. (C) Stability of HNT, NaL-HNT, and DTAB-HNT dispersions (1.1 wt%) 24 h after mixing. (D) Zeta potential (mV) measurements of HNT samples, incubated with and without E-selectin (ES), using dynamic light scattering. Data are presented as the mean ± standard deviation of three independent measurements. (E) SEM images of poly-urethane substrates with immobilized HNT samples. Scale bar = 2 μm. (F) AFM images of HNT samples immobilized on polyurethane substrates. Scale bar = 2 μm. (G) Representative surface feature height profiles of HNT samples immobilized onto polyurethane substrates, compared to smooth surfaces. Nanotube profiles have been shifted up by 100 nm for ease of viewing. (H) Root-mean-square (RMS) roughness measurements of HNT surfaces. Data are mean ± standard deviation of three independent measurements.

Approximately 1 CTC is present for every one million leukocytes in a given patient blood sample, and CTCs and leukocytes both possess similar ligands for ES. However, enhancement of HNT charge with NaL had the opposite effect on leukocyte adhesion to ES. While flowing leukocytes readily adhered to surfaces consisting of ES and HNT in the absence of surfactant (flow rate = 0.04 mL/min, WSS = 2.5 dyn/cm^2), nearly all adhesion was abolished upon enhancing HNT charge with NaL (Fig. 3D). The number of flowing leukocytes captured from flow decreased by over 90% on NaL-HNT surfaces, compared to surfaces consisting of HNT without surfactant treatment (Fig. 3E). We then performed an initial assessment of the purity of flowing cancer cells captured from a mixture of both COLO 205 cancer cells and leukocytes (flow rate = 0.04 mL/min,

WSS = 2.5 dyn/cm^2), with COLO 205:leukocyte ratios of 1:1 and 1:10. Purities as high as 90% and 75%, or enrichments as high as four- and twenty-fold, were achieved upon perfusion of cell mixtures of 1:1 and 1:10, respectively, over HNT surfaces with enhanced negative charge (Fig. 3F). Overall, these data suggest that alteration of HNT charge with NaL can induce a robust response to both enhance cancer cell capture and diminish leukocyte adhesion, both in isolation and in mixtures of cancer cells and leukocytes of varying ratios.

To assess if ES-mediated cancer cell capture and leukocyte repulsion on nanostructured surfaces is dependent on HNT charge, we functionalized HNT with DTAB surfactant to abolish the intrinsic negative charge of HNT (Fig. 1A, D). Upon perfusion of COLO 205
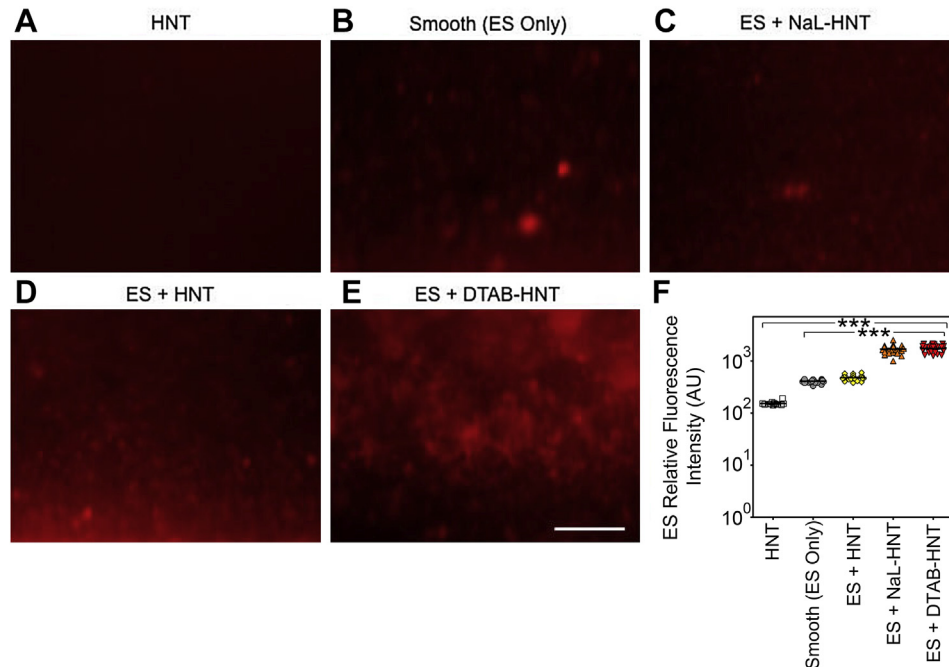
Fig. 2. Detection of immobilized fluorescent ES on biomaterial surfaces. (A–E) Representative high magnification fluorescence micrographs of recombinant human ES (red) adsorbed on immobilized HNT (control without ES; A) surfaces, smooth (ES only; B) surfaces, immobilized NaL-HNT (C), HNT (D), and DTAB-HNT (E) coated biomaterial surfaces. Scale bar = 40 μm. (F) Immobilized ES relative fluorescence intensity values on smooth and nanostructured biomaterial surfaces. Calculated values are mean ± standard deviation (n = 3). Statistics were calculated using a one-way ANOVA with Tukey post test. ***$P < 0.0001$. (For interpretation of the references to color in this figure legend, the reader is referred to the web version of this article.)
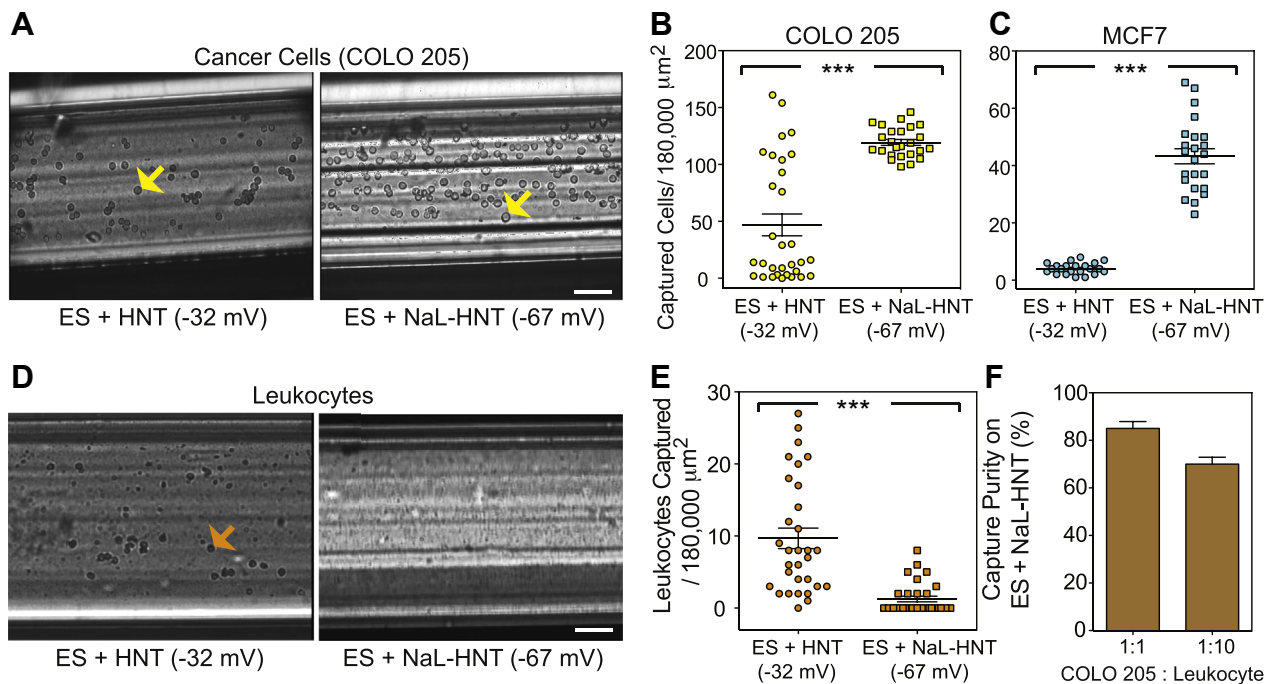

Fig. 3. Negatively charged surfactant-functionalized HNT simultaneously enhance cancer cell capture while eliminating leukocyte adhesion. (A) E-selectin (ES)-mediated adhesion of colorectal adenocarcinoma COLO 205 cells under flow over surfaces coated with ES + HNT and ES + NaL-HNT. Yellow arrows denote adhered COLO 205 cells. Scale bar = 100 μm. (B, C) Number of captured COLO 205 (B) and breast adenocarcinoma MCF7 (C) cells per 180,000 μm². n = 20 or more image frames analyzed for each condition. Statistics calculated using a two-tailed unpaired t-test. ***$P < 0.0001$. (D) ES-mediated adhesion of primary human leukocytes under flow over surfaces coated with ES + HNT and ES + NaL-HNT. Orange arrows denote adhered neutrophils. Scale bar = 50 μm. (E) Number of captured leukocytes per 180,000 μm². Calculated values are mean ± SEM. n = 20 or more image frames analyzed for each condition. Statistics calculated using a two-tailed unpaired t-test. ***$P < 0.0001$. (F) Purity (%) of COLO 205 cancer cells captured from a mixture of cancer cells and leukocytes at COLO 205:leukocyte ratios of 1:1 and 1:10. (For interpretation of the references to color in this figure legend, the reader is referred to the web version of this article.)
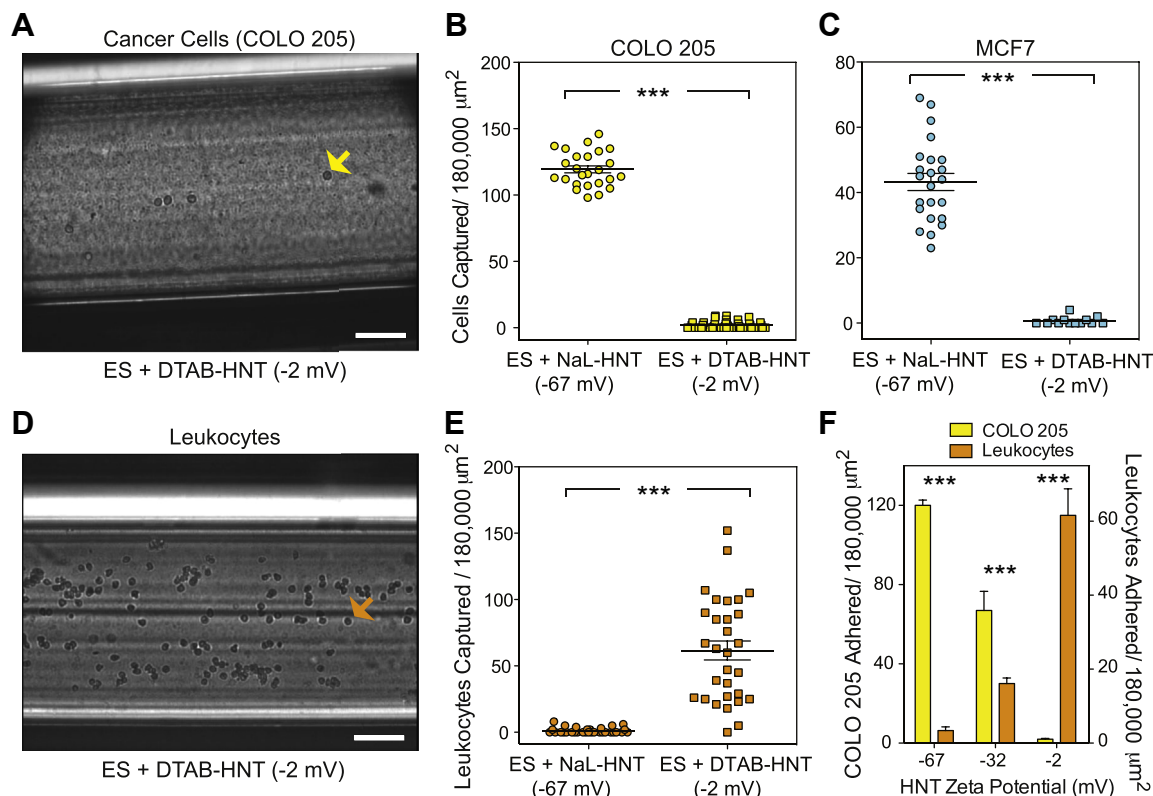
Fig. 4. HNT treatment with cationic surfactant reverses tumor cell and leukocyte capture on nanostructured biomaterial surfaces. Cancer cell and leukocyte capture on nanostructured surfaces under flow is dependent on HNT charge. (A) Negating HNT charge using DTAB surfactant abolishes cancer cell capture under flow. Yellow arrows denote adhered COLO 205 cells. Scale bar = 200 μm. (B, C) Number of captured COLO 205 (B) and MCF7 (C) cells per 180,000 μm². n = 20 or more image frames analyzed for each condition. Statistics calculated using a two-tailed unpaired t-test. ***$P < 0.0001$. (D) Negating HNT charge using DTAB surfactant restores leukocyte capture under flow. Orange arrows denote adhered leukocytes. Scale bar = 200 μm. (E) Number of captured leukocytes per 180,000 μm². Calculated values are mean ± SEM. n = 20 or more frames analyzed for captured cells for each condition. Statistics calculated using a two-tailed unpaired t-test. ***$P < 0.0001$. (F) Comparison of ES-mediated adhesion of leukocytes and COLO 205 cells per 180,000 μm² as a function of HNT zeta potential. Error bars denote standard error of the mean. Statistics were calculated using a two-tailed unpaired t-test. n = 30 or more image frames analyzed. ***$P < 0.0001$. (For interpretation of the references to color in this figure legend, the reader is referred to the web version of this article.)

cells at physiological flow rates (flow rate = 0.04 mL/min, WSS = 2.5 dyn/cm²) over surfaces consisting of ES + DTAB-HNT, it was evident that cancer cells interacted minimally with surfaces of diminished charge (Fig. 4A). The number of colon and breast cancer cells captured on DTAB-HNT surfaces of minimal charge was reduced by >99% and >97%, respectively, compared to NaL-HNT surfaces of higher negative charge (Fig. 4B, C). Leukocyte adhesion under flow, absent on HNT surfaces of higher negative charge, was enhanced on ES + DTAB-HNT of diminished charge (Fig. 4D). Dampening of negative HNT charge increased the capture of free-flowing leukocytes by 60-fold, compared to ES + NaL-HNT surfaces of higher negative charge (Fig. 4E). Plotting the number of adherent cancer cells and leukocytes as a function of HNT zeta potential shows that HNT of higher negative charge can enhance cancer cell adhesion while minimizing leukocyte adhesion, and this adhesion response can be reversed by reducing the negative charge of HNT (Fig. 4F). Taken together, these results suggest that differential ES-mediated adhesion of cancer cells and leukocytes is dependent on surfactant functionalization and charge alteration of HNT.

To assess if HNT charge can directly mediate cell interactions, the effects of surfaces consisting of charged HNT, both in the presence and absence of ES, on cancer cell firm adhesion were examined. Few COLO 205 cancer cells firmly adhered to untreated HNT in the absence of ES (Fig. 5A), while the addition of ES allowed for successful recruitment and firm adhesion of cancer cells. Interestingly, surfaces consisting of highly negatively charged NaL-

HNT alone, without ES immobilization, induced a significant increase in COLO 205 firm adhesion, compared to untreated HNT with immobilized ES. ES immobilization on NaL-HNT significantly increased COLO 205 cell firm adhesion, indicating that ES remains functional on NaL-HNT surfaces. However, given that ES only increased firm adhesion to NaL-HNT by ~15% compared to NaL-HNT alone, it appears that surfactant immobilization plays a role in recruitment of tumor cells from flow. These results indicate that HNT charge affects the adhesion of COLO 205 cancer cells to surfaces consisting of negatively charged NaL-HNT.

In an effort to exploit adhesion of tumor cells in the absence of specific adhesion ligands, the adhesion of the metastatic MDA-MB-231 breast cancer cell line to HNT-coated surfaces was examined. The MDA-MB-231 cell line is known as a "triple-negative" breast cancer (TNBC) cell type. Due to its lack of estrogen receptor, progesterone receptor, and human epidermal growth factor receptor 2 (HER2) expression, limited progress has been made in terms of therapeutic regimens for TNBC, and patients with the disease typically have the worst outcomes [47]. Additionally, MDA-MB-231 cancer cells have little to no ES ligand expression under normal culture conditions, and have been shown to engage in little to no interaction with ES and endothelial cells under flow [48,49]. Similar results were obtained in this study, as minimal MDA-MB-231 cells were found to adhesively interact with ES on HNT-coated surfaces, along with surfaces coated with untreated HNT alone (Fig. 5B, C, F). However, negatively charged NaL-HNT greatly enhanced the recruitment of MDA-MB-231 cells to the surface, both in the
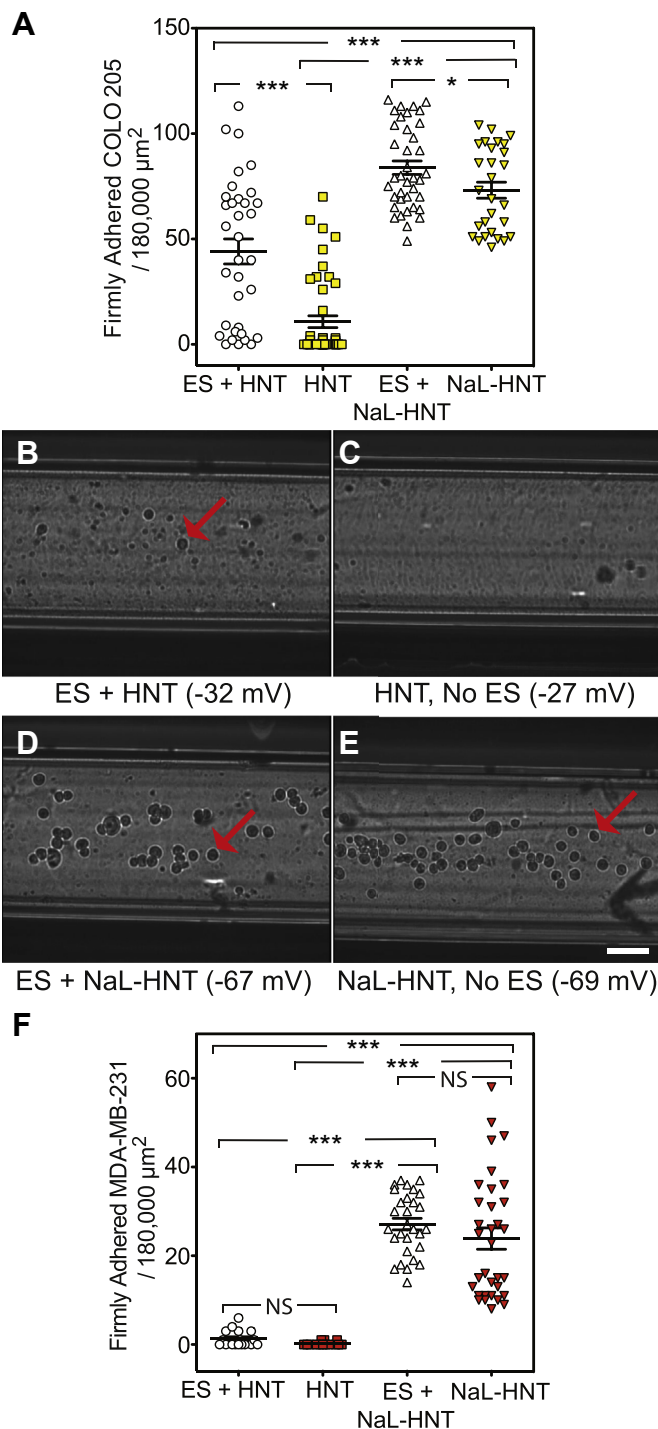
Fig. 5. NaL-HNT surfaces capture tumor cells in the absence of ES. (A) Firm adhesion of colorectal adenocarcinoma COLO 205 cells per 180,000 μm^2 to HNT and NaL-HNT in the presence and absence of the E-selectin (ES) adhesion receptor. Statistics were calculated using a one-way ANOVA with Tukey post test. ***$P < 0.0001$. *$P < 0.01$. (B–E) Comparison of triple-negative breast cancer MDA-MB-231 cell capture on HNT surfaces under flow, in presence and absence of ES adhesion proteins. Red arrows denote adhered MDA-MB-231 cells. Scale bar = 100 μm. (F) Captured MDA-MB-231 cells per 180,000 μm^2 to HNT surfaces in the presence and absence of the ES adhesion protein. Statistics calculated using a one-way ANOVA with Tukey post test. ***$P < 0.0001$. NS: not significant. (For interpretation of the references to color in this figure legend, the reader is referred to the web version of this article.)

presence and absence of ES (Fig. 5D–F). NaL-HNT induced significant increases in the number of MDA-MB-231 cells captured from flow regardless of adhesion protein immobilization (Fig. 5F). These results suggest that NaL-HNT surfaces can be utilized to capture CTCs regardless of adhesion receptor expression. While immobilization of the ES adhesion receptor can enhance the capture of cancer cells that express ES ligands, negatively charged NaL-HNT can be utilized to capture CTCs that do not express typical biomarkers or adhesion receptors.

4. Discussion

As cells approach a charged surface, the cell membrane can be either deformed toward the surface or away from it, depending on the charges present [50]. For cells expressing ES ligands, membrane deformation near charged surfaces could affect the number of cell ligands interacting with ES, and thus affect capture under flow conditions. Leukocytes have previously been reported to possess a negatively charged membrane potential [51]. Through coulombic interactions, leukocytes can be recruited to DTAB-HNT surfaces thereby enhancing ES ligation, while NaL-HNT repels leukocytes from approaching within a reactive distance to ES (Fig. 3F). Thus, it is logical that leukocytes with a high negative charge can be prevented from interacting with adhesion receptors on surfaces consisting of negatively charged HNT.

What remains to be seen is how CTC capture is enhanced on surfaces consisting of HNT of high negative charge. Few studies have examined the zeta potential of cancer cells, and have generally found that zeta potential is less negative than that of leukocytes [52,53]. The answer to enhanced cancer cell capture on NaL-HNT could lie in the CTC glycocalyx, a gel-like layer of biologically inert macromolecules on the CTC surface that can extend as far as 500 nm from the CTC surface [54]. In particular, the synthesis of glycocalyx components can be impaired during malignant transformation, causing cancer cells to greatly overexpress the glycocalyx component hyaluronan on their surface [55,56]. Additionally, leukocytes do not present a similar thick glycocalyx on surface. Thus, it is possible that components of the glycocalyx interact with NaL-HNT via electrostatic interactions, or potentially act as an adhesion ligand to the NaL surfactant. Future studies evaluating the surface charge of CTCs, and the effect of glycocalyx coatings could shed further light on the mechanisms contributing to enhanced cancer cell adhesion to charged nanostructures.

5. Conclusion

The present study demonstrates, for the first time, that simple surfactant functionalization can induce a robust, differential adhesion response of tumor cells and blood cells on nanotube-coated surfaces. Surfaces consisting of differentially charged HNT can be fabricated without significant alteration in nanostructure. Functionalization of HNT with NaL was utilized to enhance the negative charge of HNT, which resulted in a significant increase in ES-mediated cancer cell adhesion while simultaneously repelling leukocyte adhesion. In the absence of ES, NaL-HNT surfaces successfully captured metastatic cells that do not express the adhesion receptor. Conversely, diminishing HNT charge with DTAB reversed the response, abolishing cancer cell adhesion while promoting leukocyte adhesion to ES. This straightforward method to functionalize HNT with surfactants not only shows that capture of tumor cells and blood cells is dependent on HNT charge, but also provides a unique platform to isolate CTCs, from patient blood for the development of personalized medicine regimens.

Acknowledgments

References

[1] Chaffer CL, Weinberg RA. A perspective on cancer cell metastasis. Science 2011;331:1559—64.

[2] Chang YS, di Tomaso E, McDonald DM, Jones R, Jain RK, Munn LL. Mosaic blood vessels in tumors: frequency of cancer cells in contact with flowing blood. Proc Natl Acad Sci U S A 2000;97:14608—13.

[3] Butler TP, Gullino PM. Quantitation of cell shedding into efferent blood of mammary adenocarcinoma. Cancer Res 1975;35:512—6.

[4] Riethdorf S, Wikman H, Pantel K. Review: biological relevance of disseminated tumor cells in cancer patients. Int J Cancer 2008;123:1991—2006.

[5] Maheswaran S, Haber DA. Circulating tumor cells: a window into cancer biology and metastasis. Curr Opin Genet Dev 2010;20:96—9.

[6] Mitchell MJ, King MR. Fluid shear stress sensitizes cancer cells to receptor-mediated apoptosis via trimeric death receptors. New J Phys 2013;15:015008.

[7] Mitchell MJ, King MR. Computational and experimental models of cancer cell response to fluid shear stress. Front Oncol 2013;3:1—11.

[8] Coussens LM, Werb Z. Inflammation and cancer. Nature 2002;420:860—7.

[9] Lawrence MB, Springer TA. Neutrophils roll on E-selectin. J Immunol 1993;151:6339—46.

[10] McDonald B, Spicer J, Giannais B, Fallavollita L, Brodt P, Ferri L. Systemic inflammation increases cancer cell adhesion to hepatic sinusoids by neutrophil mediated mechanisms. Int J Cancer 2009;125:1298—305.

[11] van Ginhoven TM, van den Berg JW, Dik WA, Ijzermans JNM, de Bruin RWF. Preoperative dietary restriction reduces hepatic tumor load by reduced E-selectin-mediated adhesion in mice. J Surg Oncol 2010;102:348—53.

[12] Gassmann P, Kang ML, Mees ST, Haier J. In vivo tumor cell adhesion in the pulmonary microvasculature is exclusively mediated by tumor cell—endothelial cell interaction. BMC Cancer 2010;10:177.

[13] Yin X, Rana K, Ponmudi V, King MR. Knockdown of fucosyltransferase III disrupts the adhesion of circulating cancer cells to E-selectin without affecting hematopoietic cell adhesion. Carbohydr Res 2010;345:2334—42.

[14] Rahn JJ, Chow JW, Horne GJ, Mah BK, Emerman JT, Hoffman P, et al. MUC1 mediates transendothelial migration in vitro by ligating endothelial cell ICAM-1. Clin Exp Metastasis 2005;22:475—83.

[15] Mitchell MJ, Wayne E, Rana K, Schaffer CB, King MR. TRAIL-coated leukocytes that kill cancer cells in the circulation. Proc Natl Acad Sci U S A 2014;111:930—5.

[16] Mitchell MJ, King MR. Leukocytes as carriers for targeted cancer drug delivery. Expert Opin Drug Deliv 2014:1—18.

[17] Mitchell MJ, Castellanos CA, King MR. Nanostructured surfaces to target and kill circulating tumor cells while repelling leukocytes. J Nanomater 2012;2012:1—10.

[18] Mitchell MJ, King MR. Unnatural killer cells to prevent bloodborne metastasis: inspiration from biology and engineering. Expert Rev Anticancer Ther 2014;14:641—4.

[19] Hughes AD, Marshall JR, Keller E, Powderly JD, Greene BT, King MR. Differential drug responses of circulating tumor cells within patient blood. Cancer Lett 2014;352(1):28—35.

[20] Luo X, Mitra D, Sullivan RJ, Wittner BS, Kimura AM, Pan S, et al. Isolation and molecular characterization of circulating melanoma cells. Cell Rep 2014:645—53.

[21] Greene BT, Hughes AD, King MR. Circulating tumor cells: the substrate of personalized medicine? Front Oncol 2012;2:1—6.

[22] Allard WJ, Matera J, Miller MC, Repollet M, Connelly MC, Rao C, et al. Tumor cells circulate in the peripheral blood of all major carcinomas but not in healthy subjects or patients with nonmalignant diseases. Clin Cancer Res 2004;10:6897—904.

[23] Yu M, Stott S, Toner M, Maheswaran S, Haber DA. Circulating tumor cells: approaches to isolation and characterization. J Cell Biol 2011;192:373—82.

[24] Miller MC, Doyle GV, Terstappen LWMM. Significance of circulating tumor cells detected by the CellSearch system in patients with metastatic breast colorectal and prostate cancer. J Oncol 2010;2010:617421.

[25] Nagrath S, Sequist LV, Maheswaran S, Bell DW, Irimia D, Ulkus L, et al. Isolation of rare circulating tumour cells in cancer patients by microchip technology. Nature 2007;450:1235—9.

[26] Hughes AD, Mattison J, Western LT, Powderly JD, Greene BT, King MR. Microtube device for selectin-mediated capture of viable circulating tumor cells from blood. Clin Chem 2012;58:846—53.

[27] Bajpai S, Mitchell MJ, King MR, Reinhart-King CA. A microfluidic device to select for cells based on chemotactic phenotype. Technology 2014;02:101—5.

[28] Mitchell MJ, Chen CS, Ponmudi V, Hughes AD, King MR. E-selectin liposomal and nanotube-targeted delivery of doxorubicin to circulating tumor cells. J Control Release 2012;160:609—17.

[29] Liu M, Guo B, Du M, Cai X, Jia D. Properties of halloysite nanotube—epoxy resin hybrids and the interfacial reactions in the systems. Nanotechnology 2007;18:455703.

[30] Abdullayev E, Joshi A, Wei W, Zhao Y, Lvov Y. Enlargement of halloysite clay nanotube lumen by selective etching of aluminum oxide. ACS Nano 2012;6:7216—26.

[31] Lvov YM, Shchukin DG, Möhwald H, Price RR. Halloysite clay nanotubes for controlled release of protective agents. ACS Nano 2008;2:814—20.

[32] Veerabadran NG, Price RR, Lvov YM. Clay nanotubes for encapsulation and sustained release of drugs. Nano 2007;02:115—20.

[33] Cavallaro G, Lazzara G, Milioto S. Exploiting the colloidal stability and solubilization ability of clay nanotubes/ionic surfactant hybrid nanomaterials. J Phys Chem C 2012;116:21932—8.

[34] Hughes AD, King MR. Use of naturally occurring halloysite nanotubes for enhanced capture of flowing cells. Langmuir 2010;26:12155—64.

[35] Mitchell MJ, King MR. Shear-induced resistance to neutrophil activation via the formyl peptide receptor. Biophys J 2012;102:1804—14.

[36] Mitchell MJ, Lin KS, King MR. Fluid shear stress increases neutrophil activation via platelet-activating factor. Biophys J 2014;106:2243—53.

[37] Horcas I, Fernández R, Gómez-Rodríguez JM, Colchero J, Gómez-Herrero J, Baro AM. WSXM: a software for scanning probe microscopy and a tool for nanotechnology. Rev Sci Instrum 2007;78:013705.

[38] Silberberg MS. Chemistry: the molecular nature of matter and change. 5th ed. McGraw Hill; 2008.

[39] Chen W, Weng S, Zhang F, Allen S, Li X, Bao L, et al. Nanoroughened surfaces for efficient capture of circulating tumor cells without using capture antibodies. ACS Nano 2013;7:566—75.

[40] Ball C, King M. Role of c-Abl in L-selectin shedding from the neutrophil surface. Blood Cells Mol Dis 2011;46:246—51.

[41] Cao TM, Mitchell MJ, Liesveld J, King MR. Stem cell enrichment with selectin receptors: mimicking the ph environment of trauma. Sensors 2013;13:12516—26.

[42] Kim MB, Sarelius IH. Distributions of wall shear stress in venular convergences of mouse cremaster muscle. Microcirculation 2003;10:167—78.

[43] Myung JH, Gajjar KA, Pearson RM, Launiere CA, Eddington DT, Hong S. Direct measurements on CD24-mediated rolling of human breast cancer MCF-7 cells on E-selectin. Anal Chem 2011;83:1078—83.

[44] Shafie SM, Liotta LA. Formation of metastasis by human breast carcinoma cells (MCF-7) in nude mice. Cancer Lett 1980;11:81—7.

[45] Mattila MM-T, Ruohola JK, Karpanen T, Jackson DG, Alitalo K, Härkönen PL. VEGF-C induced lymphangiogenesis is associated with lymph node metastasis in orthotopic MCF-7 tumors. Int J Cancer 2002;98:946—51.

[46] Kawada K, Hosogi H, Sonoshita M, Sakashita H, Manabe T, Shimahara Y, et al. Chemokine receptor CXCR3 promotes colon cancer metastasis to lymph nodes. Oncogene 2007;26:4679—88.

[47] Tate CR, Rhodes LV, Segar HC, Driver JL. Targeting triple-negative breast cancer cells with the histone deacetylase inhibitor panobinostat. Breast Cancer Res 2012;14:R79.

[48] Julien S, Ivetić A, Grigoriadis A, QiZe D, Burford B, Sproviero D, et al. Selectin ligand sialyl-Lewis x antigen drives metastasis of hormone-dependent breast cancers. Cancer Res 2011;71:7683—93.

[49] Evani SJ, Prabhu RG, Gnanaruban V, Finol EA, Ramasubramanian AK. Monocytes mediate metastatic breast tumor cell adhesion to endothelium under flow. FASEB J 2013;27:3017—29.

[50] Vorobyov I, Bekker B, Allen TW. Electrostatics of deformable lipid membranes. Biophys J 2010;98:2904—13.

[51] Parodi A, Quattrocchi N, van de Ven AL, Chiappini C, Evangelopoulos M, Martinez JO, et al. Synthetic nanoparticles functionalized with biomimetic leukocyte membranes possess cell-like functions. Nat Nanotechnol 2012;8:61—8.

[52] Zhang Y, Yang M, Park J-H, Singelyn J, Ma H, Sailor MJ, et al. A surface-charge study on cellular-uptake behavior of F3-peptide-conjugated iron oxide nanoparticles. Small 2009;5:1990—6.

[53] Zhang Y, Yang M, Portney NG, Cui D, Budak G, Ozbay E, et al. Zeta potential: a surface electrical characteristic to probe the interaction of nanoparticles with normal and cancer human breast epithelial cells. Biomed Microdevices 2008;10:321—8.

[54] Mitchell MJ, King MR. Theme: physical biology in cancer. 3. The role of cell glycocalyx in vascular transport of circulating tumor cells. AJP Cell Physiol 2014;306:C89—97.

[55] Hopwood JJ, Dorfman A. Glycosaminoglycan synthesis by cultured human skin fibroblasts after transformation with simian virus 40. J Biol Chem 1977;252:4777—85.

[56] Itano N, Kimata K. Altered hyaluronan biosynthesis in cancer progression. Semin Cancer Biol 2008;18:268—74.